Frontal changes in the Manimahesh and Tal Glaciers in the Ravi basin, Himachal Pradesh, northwestern Himalaya (India), between 1971 and 2013

Article *in* International Journal of Remote Sensing · August 2015

DOI: 10.1080/01431161.2015.1074300

2 authors:

Pritam Chand
Central University of Punjab

Milap C Sharma
Jawaharlal Nehru University

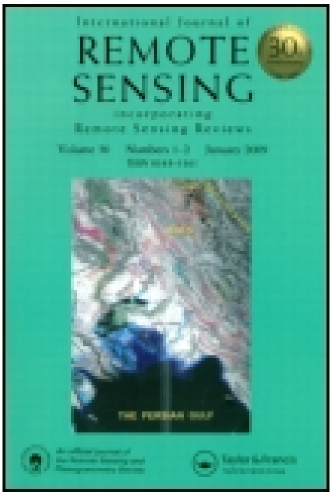

International Journal of Remote Sensing
Publication details, including instructions for authors and subscription information:
http://www.tandfonline.com/loi/tres20

Frontal changes in the Manimahesh and Tal Glaciers in the Ravi basin, Himachal Pradesh, northwestern Himalaya (India), between 1971 and 2013

Pritam Chand[a] & Milap Chand Sharma[a]
[a] Centre for the Study of Regional Development (CSRD), SSS New Building, Jawaharlal Nehru University (JNU), New Delhi 110067, India
Published online: 14 Aug 2015.

International Journal of Remote Sensing, 2015
Vol. 36, No. 16, 4095–4113, http://dx.doi.org/10.1080/01431161.2015.1074300

Taylor & Francis
Taylor & Francis Group

Frontal changes in the Manimahesh and Tal Glaciers in the Ravi basin, Himachal Pradesh, northwestern Himalaya (India), between 1971 and 2013

Pritam Chand* and Milap Chand Sharma

Centre for the Study of Regional Development (CSRD), SSS New Building, Jawaharlal Nehru University (JNU), New Delhi 110067, India

(*Received 20 February 2015; accepted 15 July 2015*)

The Manimahesh and Tal Glaciers are located in the Budhil fifth-order sub-basin of the Ravi, Himachal Himalaya, Northwestern Himalaya (India). These glaciers were analysed using high- (Corona KH-4A) to medium- (Landsat TM/ETM+/OLI, ASTER) spatial resolution satellite data between 1971 and 2013, along with extensive field measurements (2011–2014) of frontal changes. The results show that the Manimahesh and Tal Glaciers retreated by 157 ± 34 m (4 ± 1 m year^{-1}) and 45 ± 34 m (1 ± 1 m year^{-1}), respectively, whereas, the total area lost is estimated at 0.21 ± 0.01 km^2 (0.005 km^2 year^{-1}) and 0.010 ± 0.003 km^2 (0.0002 km^2 year^{-1}), respectively, between 1971 and 2013. The rate of retreat is significantly lower than that previously reported. Our field measurements (2011–2014) also suggest a retreating trend and validate the measured glacier changes using remotely sensed temporal data.

1. Introduction

As an integral part of the cryosphere, mountain glaciers constitute one of the most important components of the Earth's natural system (Slaymaker and Kelly 2007). Moreover, the Himalaya–Karakoram (H-K) region has the largest concentration of glaciers outside the polar region and has exhibited a receding trend since the end of the Little Ice Age (LIA), with some exceptions of long-term irregular behaviour of glacier dynamics with frequent advances and possible slight mass gain in Karakorum Himalaya (Mayewski and Jeschke 1979; Bolch et al. 2012; Gardelle et al. 2013; Hewitt 2011; Kääb et al. 2012). However, current knowledge on the behaviour of glaciers in the Himalayan region is limited (Bolch et al. 2012). Continuous long-term monitoring can improve our knowledge on glacial response to climate change in the less-studied regions of the Himalayan region. Most previous glacier studies were based on terminus monitoring for the Indian Himalaya (Kulkarni et al. 2007; Mir et al. 2014; Pandey and Venkataraman 2013; Pandey, Ghosh, and Nathawat 2011; Kulkarni and Rathore 2005; Mehta, Dobhal, and Bisht 2011; Mehta et al. 2014). Most of these used either the Survey of India (SoI) topographic maps or coarser-resolution satellite data sets (e.g. Landsat MSS), but some used high-resolution Corona images (Bhambri et al. 2011, 2013; Bhambri, Bolch, and Chaujar 2012; Negi et al. 2013). Although field-based mass balance and glacier area change measurements are highly recommended, and given their size, altitude, and difficult terrain, only a limited number of glaciers have been investigated in the field in terms of glacier terminus change measurements and mass balance studies (Azam et al. 2012; Dobhal, Mehta, and

*Corresponding author. Email: pritamiirs@gmail.com

Srivastava 2013). In particular, change in glacier terminus shows an integrated behaviour reflecting climatic conditions (mainly temperature and precipitation) on a long-term basis, persisting over many years and easy to measure, and is available for many glaciers globally (Zemp et al. 2008). These records are useful to reconstruct glacier mass balance; estimate glacier contribution to sea-level rise; historical equilibrium-line altitudes; response times of glaciers; and evidence of past and ongoing climatic variations along with shifting trends (Paul and Svoboda 2009). With these considerations and acknowledging the potential significance of glaciers and their dynamics, high-resolution remote-sensing and *in situ* measurements of glacier snout positions and surface area changes were carried out for the Manimahesh and Tal Glaciers in the Ravi basin, Himachal Himalaya. In 2005, the Geological Survey of India (GSI; Shukla and Dutta 2005) carried out change measurement studies for these glaciers using SoI topographical maps as a historical reference for glacial extent (1960s) and linear retreat. SoI topographic maps represent an important database for historical information on land-cover characteristics, with highly accurate topographical detail. However, the mapped Himalayan glacier features on SoI topographical maps (earlier maps and 1960s–70s updated maps) were validated with limited fieldwork due to restricted accessibility, high altitude, and difficult terrain in the glaciated areas, and to inaccuracies in representation of glacial features on SoI topographical maps reported by earlier surveyors (e.g. Mason (Bhambri, Bolch, and Chaujar 2010)). Furthermore, due to seasonal snow cover, it is difficult to identify the glacier terminus and boundary accurately from late or early winter aerial photographs as were used for updating the SoI topographic maps in the 1960s–70s (Raina and Srivastava 2008; Bhambri and Bolch 2009). Moreover, recent studies have shown inaccuracies in SoI topographical maps in terms of snout positions (Bhambri and Bolch 2009). Thus, declassified high-spatial resolution imagery (e.g. Corona and Hexagon) from the 1960s and 1970s is a reliable data set for mapping the historic extent of glaciers for almost the same period as the updated SoI topographical maps, and can also be used for comparison of glacier outlines derived from older SoI topography maps (Bolch et al. 2010; Bhambri et al. 2011; Bhambri, Bolch, and Chaujar 2012; Bolch et al. 2008). These images are accessible from the United States Geological Survey (USGS) website (http://earthexplorer.usgs.gov/). However, to the best of our knowledge, there have been no previous attempts to measure the length data of the Manimahesh and Tal Glaciers from historic high-resolution Corona images, or to assess the accuracy of glacier boundaries marked on SoI topographic maps. Therefore, this study has two objectives: (1) to assess and re-examine changes in the Manimahesh and Tal Glaciers terminus and area between 1971 and 2013 using high-resolution declassified images and recent field measurements; and (2) to assess the suitability of SoI topographic maps for the mapping of historical glacier outlines and their change.

2. Regional and climatic characteristics of the study area

The Ravi basin is located in the southeastern part of Chamba district and northeastern part of Kangra district in Himachal Himalaya (India). It covers three sub-basins – Siul, Budhil, and Upper Ravi (Figure 1). The Manimahesh and Tal Glaciers are located in the Budhil sub-basin of the Ravi, in the Bharmour subdivision of Chamba district, Himachal Pradesh (India). The geographical extent of the Budhil sub-basin lies between 32° 40′ 1.2″ N and 32° 21′ 28.8″ N, and 76° 24′ E and 76° 53′ 2.4″ E, covered by SoI topographic map numbers 52 D/11 and 15 (Figure 1(*a*)). The Budhil River, downstream of Kugti, flows through a deep incision which at places attains the formation of a gorge. This can be

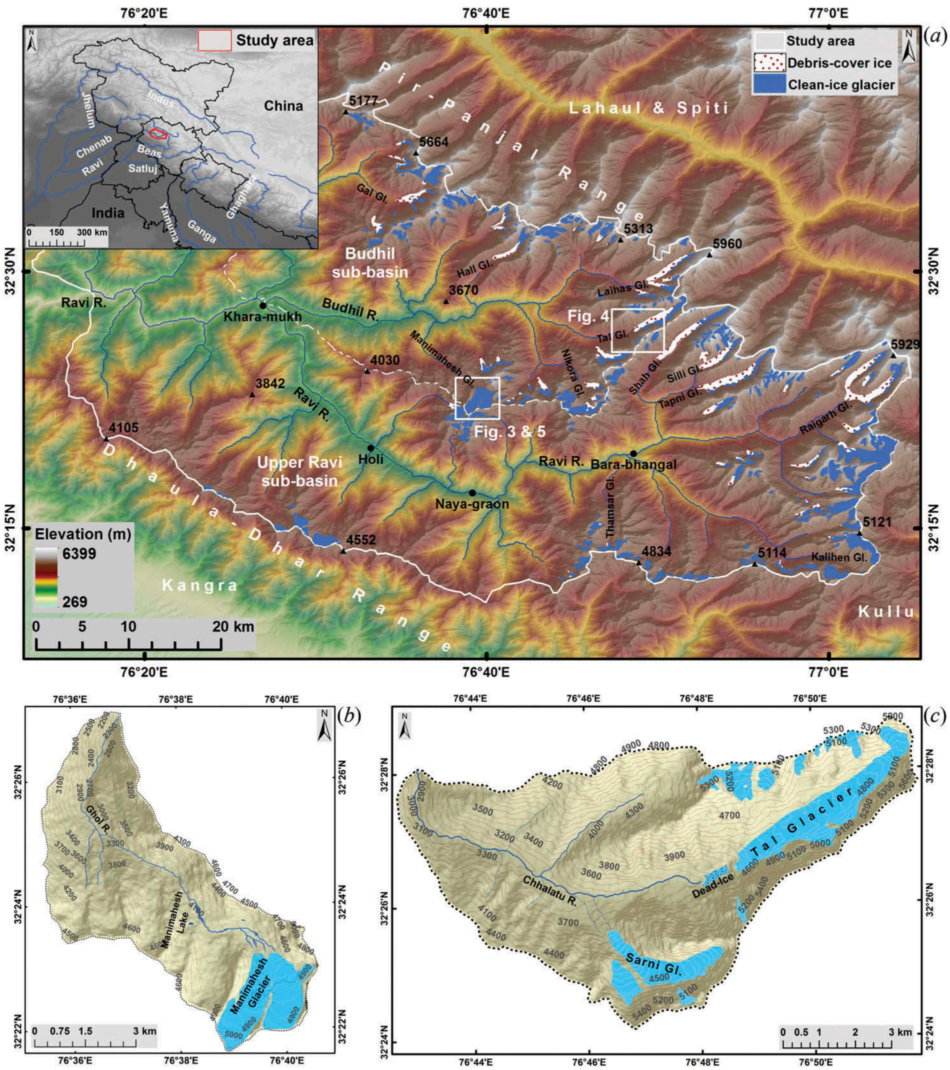

Figure 1. Location of study glaciers. (*a*) Location of glaciers in the Ravi basin, Himachal Himalaya; (*b*) Manimahesh Glacier and its valley morphology; (*c*) Tal Glacier and its valley morphology.

attributed to uplifting and neo-tectonic activity (Shukla and Dutta 2005). The total upper basin area covers about 850 km^2 with altitude in the range 1400–6000 m a.s.l.

The climate of the study area is transitional between the dry winter climate of the Indo-Gangetic plains (CWg according to Koppen's classification) and the highland climate (H) of the Western Himalaya (Spate and Learmonth 1967). The basin lies between the transition zone of the maximum (Dharamshala) and minimum (Lahaul) precipitation areas of Himachal Pradesh (Figure 2). Bharmour (about 2150 m a.s.l.), a small town located in the Pir-Panjal ranges, experienced an annual average of 1180 mm precipitation during the period 1975–2000 (Bhagat et al. 2004). The Indian summer monsoon (June–September) accounted for 56.9% (486.4 mm year^{-1}) of the average annual rainfall, while

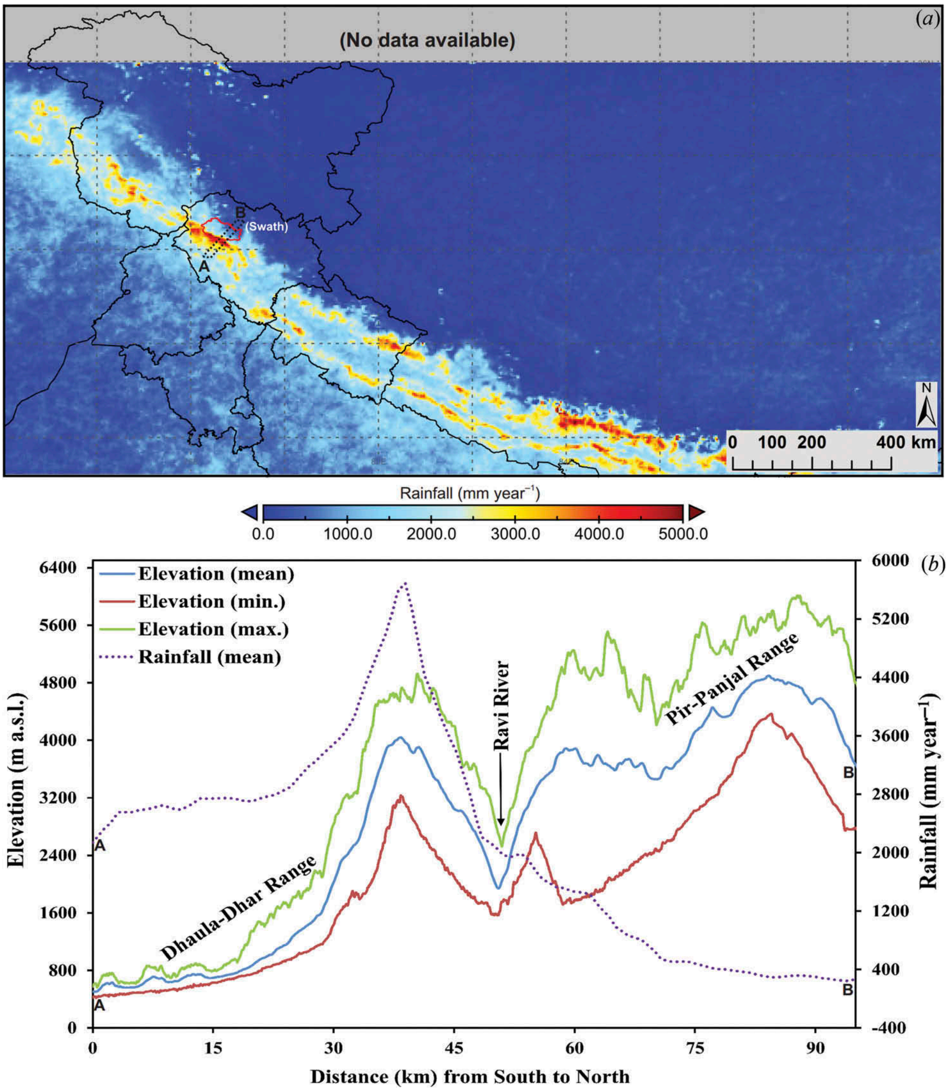

Figure 2. Precipitation gradient (1998–2010) for northwestern Himalaya (data source: TRMM 2B31, http://www.geog.ucsb.edu/~bodo/TRMM/index.php). (*a*) Spatial distribution of annual rainfall for northwestern Himalaya; (*b*) simple topography–rainfall relationship from south to north (15 km swath, A–B) for the Ravi basin.

mid-latitude westerlies (November–March) contributed 32.4% (278.5 mm year^{-1}) as recorded during 1990–2013 for the Chamba Indian Meteorological (IMD) station (Pareta and Pareta 2014). This suggests that the glaciers of Ravi basin are mainly influenced by the Indian summer monsoon, and co-dominantly, by the winter mid-latitude westerlies which contribute significantly. Owing to large differences in elevation and respective temperatures, the seasonal snowline is highly variable, decreasing to an elevation of about 2000 m a.s.l. during winter and retreating to above 4500 m a.s.l. in summer.

The Manimahesh Glacier (32° 22′ 30″ N and 76° 40′ 4.8″ E) is a mountain-type glacier; in 2013, it was recorded as having a clean ice cover of area and length

Table 1. Retreat of Manimahesh and Tal Glaciers measured by GSI in 2005.

Glacier	Period	Terminus change		Area change	
		Total (m)	Rate of retreat (m $year^{-1}$)	Total (km^2)	Loss (km^2 $year^{-1}$)
Manimahesh	1968–2005	1075	29.05	0.68	0.02
Tal	1963–2005	1675	39.88	0.71	0.02

4.3 ± 0.1 km^2 and approximately 3.2 ± 0.03 km, respectively (Figure 1(*b*)). The Tal Glacier (32° 27′ 46.8″ N and 76° 50′ 56.4″ E) is a valley glacier; in 2013, it was recorded as having extensive debris covering 47.1 ± 1% of the total area (4.4 ± 0.1 km^2), and its length was approximately 6.1 ± 0.03 km for year 2013 (Figure 1(*c*)). These two glaciers can be considered as representative of that area in terms of morphology and surface cover. Thus, changes in the multi-temporal glacier frontal area and terminus for these two representative glaciers mirror glacial fluctuation between 1971 and 2013 in the Budhil sub-basin of Ravi. These glaciers were studied in 2005 by GSI using SoI topographic maps as a source of historical data (Shukla and Dutta 2005; Table 1).

3. Data sets and methodology

3.1. Data sets

The present study used 1970s declassified high-resolution Corona KH-4A (1971) satellite images to widen the time span for monitoring the historic extent of the glacier back, and this conceivably provides more consistent results than SoI topographic maps and coarse-resolution satellite data sets (Bhambri et al. 2011; Bhambri, Bolch, and Chaujar 2012). Orthorectified Landsat ETM+ (2002) and Landsat 8 OLI (2013) medium spatial resolution images were used for mapping glacier terminus and area changes in the 2000s and present, respectively (Table 2). In addition, the availability of high-resolution images from Google Earth (GE; 2013) and Bhuvan-2D/3D (http://bhuvan.nrsc.gov.in/bhuvan_links.php) allowed us to identify and map the glacier terminus with suitable accuracy for recent years, supplemented by field measurements. Furthermore, an ASTER (2002) image with a different swath and areal coverage was also used to assist in identifying the glacier terminus from Landsat ETM+ Pan (2002). A Landsat TM image (1989) was used for mapping the position of the glacier terminus in the 1990s. Most of the data sets were selected for the end of the ablation period with minimum seasonal snow cover and a high solar position, to avoid deep shadows (Paul and Svoboda 2009). The Landsat ETM+ Pan imagery was used as base image for rectification of older Corona KH-4A and other temporal images. Most of the Corona KH-4A image strips used to investigate glacial change in the Ravi basin were situated near the nadir point, which minimized distortion in terms of the area on the extremity of the strip (Beck et al. 2007). A spline adjustment method inbuilt in ESRI ArcGIS 10.1 was used as a geo-referencing method for Corona images to provide results within acceptable error (<15 m; Bhambri et al. 2011). Fifty ground control points (GCPs) were acquired from Landsat ETM+ Pan imagery for co-registration. In addition, 40 GCPs (with planimetric accuracy (*x, y*) of ±3 m), collected during field expeditions in 2011–2014 using a non-differential global positioning system (GPS, Garmin GPSMAP 76Cx ± 5–10 m), were used initially for rectification and to further minimize the overall rectification error. GCPs were selected based on stream junctions, edges of rocky outcrops, stable peaks, established field corners, and prominent

Table 2. Data used in the present study.

Satellite/sensor	Date of acquisition	Spatial resolution (m)	Scene ID	Accuracy RMSE (x,y) (m)
Corona KH-4B	28 September 1971	3	70 MM X DS1115-2282DA068	~5.3
		3	70 MM X DS1115-2282DF062	
Landsat 5 TM	9 October 1989	30, 60	ETP147R37_5T19891009/ETP147R38_5T19891009	~7.8
Landsat 7 ETM+	2 August 2002	15, 30, 60	LE71470372002214SGS00	Base image
ASTER	28 October 2002	15, 30, 90	AST_L1A_003_10282002054845_11112002172853	~7.2
Landsat 8 OLI/TRIS	25 September 2013	15, 30, 100	LC81470382013268LGN00	~5.4
	27 October 2013	15, 30, 100	LC81470382013300LGN00	~5.4

linear geological structure (e.g. lineaments). Additionally, non-orthorectified Landsat TM (1989) and ASTER (2002) images were rectified using the projective transformation algorithm inbuilt in the AutoSync tool of Erdas Imagine 10 by incorporating ASTER GDEM V2. SoI topographic maps 52 D 11 and 15 (at 1:50,000 scale with 40 m contour interval (planimetric accuracy ±12.5 m and elevation accuracy ±6.5 m; Raju and Ghosh 2003)) were used for comparison and extraction of glacier outlines from the SoI topographic maps (1963 and 1968) and the high-resolution Corona image (1971).

3.2. Glacier mapping, changes, and uncertainty estimation

The classification of the Global Land Ice Measurements from Space (GLIMS) initiatives (http://www.glims.org/MapsAndDocs/guides.html) was adopted to map the glacier boundaries from satellite images. The glacier clean-ice-covered areas were mapped from Landsat images (1990s–2013) using the well-established semi-automated band ratio method (i.e. the ratio $B_{\mathrm{Red}}/B_{\mathrm{SWIR\text{-}I}}$, where B is the spectral band, and B_{Red} and $B_{\mathrm{SWIR\text{-}I}}$ represent the red band and first shortwave infra-red band (SWIR-I), respectively), followed by a 3 × 3 median filter (Bolch, Menounos, and Wheate 2010; Racoviteanu, Williams, and Barry 2008; Bhambri et al. 2013; Frey, Paul, and Strozzi 2012). A 3 × 3 median filter helps to smooth the resulting glacier outlines and removes noise in regions of shadow or from small, isolated snow patches (Racoviteanu et al. 2009). However, this ratio method misclassified lakes, seasonal snow cover, and ice on water, and was further manually corrected using contrast-enhanced false-colour composites of the respective satellite scenes in the background (Paul, Frey, and Le Bris 2011). Additionally, glacier ice under optically thick debris cover is not mapped by this method. Therefore, the debris-covered area from multispectral images (e.g. Landsat TM/ETM+/OLI) and glacial extent from panchromatic Corona KH-4A images (1971) were manually delineated. Moreover, the Landsat ETM+/OLI multispectral images (30 m) were merged with the high-resolution Pan images (15 m) using the Brovey transform image fusion technique (Csatho, Van Der Veen, and Tremper 2005). Pan-sharpened multispectral images help to determine the most likely position of the glacier termini, based on signs of movement (identified by overlays of multi-temporal images); emerging melt water streams at the end of the terminus; spectral colour differences; and the presence of small melt water ponds (Bhambri et al. 2013).

The change in glacier length was calculated by drawing parallel line stripes at intervals of 25 m. This was calculated as the average length from the intersection of the stripes with the glacier outlines and further along the central flow line for comparison with average length change (Bhambri, Bolch, and Chaujar 2012). During field expeditions, permanent reference stations previously established by GSI in 2005 were identified and the same geographical positions recorded in the GPS; thereafter, the terminus positions were measured by a Bushnell hand-held laser distance meter (LDM, with an accuracy of ±1 m) and saved as GPS tracks in the accessible area. Geographical positions of each reference station, measured distances, and the saved tracks were transferred to recent satellite images for change analysis.

The present study used multi-temporal data sets and deserves proper consideration to ascertain the accuracy and significance of the results. Previous studies report a mapping uncertainty of ±2–5% for clean ice glaciers (Paul et al. 2002), while under perfect conditions some achieved lower than half-pixel accuracy (Bolch et al. 2010). Glacier mapping uncertainty was estimated using the buffer method, based on buffering around the glacier margins, as suggested by Granshaw and Fountain (2006). The buffer size selected was half of the estimated shift caused by misregistration, as only one side can be affected by the shift (Bolch et al., 2010). The buffer size was set to 7.5 m for the Landsat 7 ETM+ and Landsat 8 OLI images, whereas for Landsat TM it was set to 15 m. A smaller buffer size of 2.5 m was used for the Corona by taking the image resolution and positional accuracy (5.3 m) into account. Accordingly, the average mapping uncertainty was 0.8%, 4.5%, 2.3%, and 2.5% for Corona (1971), Landsat TM (1989), Landsat ETM+, and Landsat 8 OLI (2013) images, respectively. Furthermore, uncertainty was evaluated by comparing glacier outlines derived from multispectral bands with 30 m resolution of a 2013 Landsat 8 OLI image, and those derived from a high-resolution GE image of the same year for Tal Glacier, as suggested by Paul et al. (2013). The resultant uncertainty was ±3.1%, which is within the range of the above-mentioned uncertainty and those reported by previous studies (around 2–5%; Bhambri et al. 2013; Paul et al. 2013). The spline method and projective transformation algorithm provide better registration with a minimum error (Bhambri et al. 2011). In addition, to assess positional accuracy, 24 common location points such as stable river junctions and peaks were identified in both the Landsat ETM+ Pan (2002) and Corona images (1971). The horizontal shift between both images was 5.3 m (1.8 pixels). The co-registration error for Landsat TM was 7.8 m, and for Landsat 8 OLI was 5.4 m, with reference to the base image of Landsat ETM+ Pan (2002). This study used glacier length change uncertainty (e in Equation (1)), as suggested by Hall et al. (2003):

$$e = \sqrt{{a_1}^2 + {a_2}^2} + E_{\text{reg}}, \tag{1}$$

where a_1 and a_2 are the pixel resolution of images 1 and 2, respectively, and E_{reg} is the registration error. Accordingly, the uncertainty calculated for Corona (1971), Landsat TM (1989), and Landsat 8 OLI (2013) was 20.6, 41.3, and 26.6 m, respectively. The uncertainty for glacial area change was estimated by multiplication of the uncertainty of glacier length with the glacier width (Bhambri, Bolch, and Chaujar 2012).

4. Results

The study measured the average recession of the Manimahesh Glacier between 1971 and 2013 as approximately 157 ± 34 m, with an annual average rate of 4 ± 1 m. The total area vacated by the Manimahesh Glacier during the same period is estimated at 0.21 ± 0.01 km^2, with an annual average rate of 0.0050 ± 0.0002 km^2, representing approximately 4.6% of the total loss. During the period 1971–1989, Manimahesh Glacier lost an area of 0.07 ± 0.01 km^2 with average retreat of 51 ± 46 m (3 ± 3 m $year^{-1}$), which increased to 63 ± 47 m (5 ± 4 m $year^{-1}$) with an areal loss of 0.10 ± 0.01 km^2 in the period 1989–2002. The average recession rate declined between 2002 and 2013 to 43 ± 34 m (4 ± 3 m $year^{-1}$), with an areal loss of 0.030 ± 0.004 km^2 (Figure 3; Tables 3 and 4). The debris-covered Tal Glacier showed no significant change during the period 1971–2013, with a total average terminus retreat of 45 ± 34 m and areal loss of 0.010 ± 0.003 km^2 (Figure 4; Tables 3 and 4). GSI investigation in 2005 using SoI topography maps (1963 and 1968) as historical data sets and field measurements thereof show higher recession than the present assessed rate for these glaciers. For instance, GSI reported that the Manimahesh and Tal Glaciers had receded by 1075 m (29 m $year^{-1}$) and 1675 m (40 m $year^{-1}$), respectively, during the periods 1968–2005 and 1963–2005. The total area vacated by the Manimahesh and Tal Glaciers was estimated at 0.68 km^2 (0.02 km^2

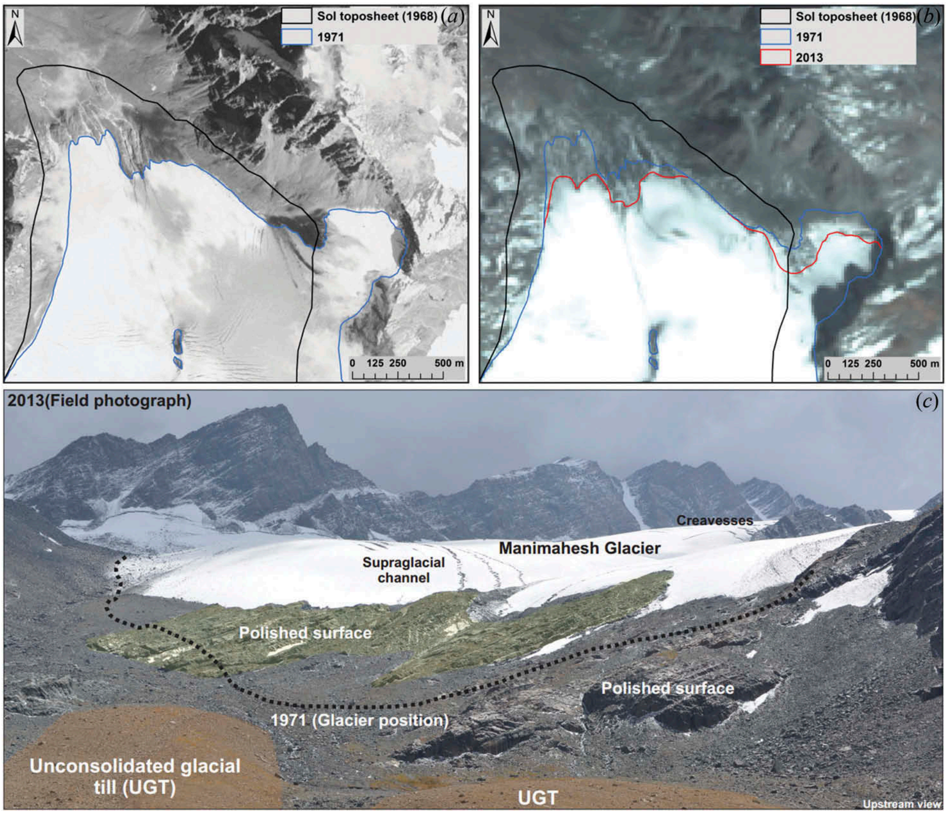

Figure 3. Recession of Manimahesh Glacier, Budhil sub-basin of Ravi. (*a*) Corona KH-4A image (28 September 1971) with same-year glacier outline; (*b*) Landsat 8 OLI Pan image (27 September 2013) with glacier outline for 1971 and 2013; (*c*) field photograph (2013) of Manimahesh Glacier, and its deglaciated area in the foreground.

year^{-1}) and 0.70 km^2 (0.02 km^2 year^{-1}), respectively, for these by two periods by GSI in 2005 (Shukla and Dutta 2005). As per the 2005 GSI report, Tal Glacier had not only thinned but the lower part became detached from the main glacier body from 1963, based on SoI maps. However, the Corona (1971) image suggests that there had been minute changes and the glacier retained two identifiable bodies – one active and the other as detached dead ice. This fact is further reinforced by both a field survey (2013) and multi-temporal satellite images of Corona (1971), Landsat ETM (2002), Landsat 8 OLI (2013), and GE (2013) images (Figure 4). The average recession rate for the detached lower dead ice part of the former glacier was estimated at 304 ± 34 m (7 ± 1 m year^{-1}), with a total areal loss of 0.09 ± 0.01 km^2 between 1971 and 2013 (Figure 4; Tables 3 and 4). This dead ice body is supported by ice and snow avalanching from the snout of the upper main glacier trunk and adjoining steep slopes, covered by supraglacial debris which acts as an insulator and protects the ice from rapid melting, as has been reported in adjoining Lahual Himalaya (e.g. at Rawling glacier *née* Ralling) by Benn and Owen (2002). Such features are difficult to identify from satellite-based differentiations unless supported by either proper field authentication or higher-resolution data with no seasonal snow cover.

International Journal of Remote Sensing 2015.36:4095-4113.

Table 3. Total areal loss at the end of the study periods for Manimahesh Glacier, Tal Glacier, and the dead ice part of Tal Glacier.

	Manimahesh		Tal		Dead ice part	
Years	Total (10^3 m^2)	Rate of loss (10^3 m^2 $year^{-1}$)	Total (10^3 m^2)	Rate of loss (10^3 m^2 $year^{-1}$)	Total (10^3 m^2)	Rate of loss (10^3 m^2 $year^{-1}$)
1971–1989	72.2 (±5.7)	4.0 (±0.3)	–	–	38.5 (±5.2)	2.1 (±0.3)
1989–2002	104.1 (±7.2)	8.0 (±0.6)	–	–	17.7 (±3.6)	1.4 (±0.3)
2002–2013	34.6 (±4.4)	3.1 (±0.4)	–	–	30.9 (±4.2)	2.8 (±0.4)
Total (1971–2013)	210.9 (±8.9)	5.0 (±0.2)	10.0 (±3.5)	0.20 (±0.08)	87.1 (±6.6)	2.1 (±0.2)

Table 4. Total and average recession of Manimahesh Glacier, Tal Glacier, and dead ice part of Tal Glacier.

	Manimahesh			Tal			Dead ice part		
Years	Total average retreat (m)	Rate of retreat (m $year^{-1}$)	Total retreat (along central flow line) (m)	Total average retreat (m)	Rate of retreat (m $year^{-1}$)	Total retreat (along central flow line) (m)	Total average retreat (m)	Rate of retreat (m $year^{-1}$)	Total retreat (along central flow line) (m)
1971–1989	51 (±46)	3 (±3)	78 (±46)	–	–	–	138 (±46)	8 (±3)	91 (±46)
1989–2002	63 (±47)	5 (±4)	79 (±47)	–	–	–	72 (±47)	6 (±4)	73 (±47)
2002–2013	43 (±34)	4 (±3)	56 (±34)	–	–	–	95 (±34)	9 (±3)	127 (±34)
Total (1971–2013)	157 (±34)	4 (±1)	212 (±34)	45 (±34)	1 (±1)	85 (±34)	304 (±34)	7 (±1)	290 (±34)

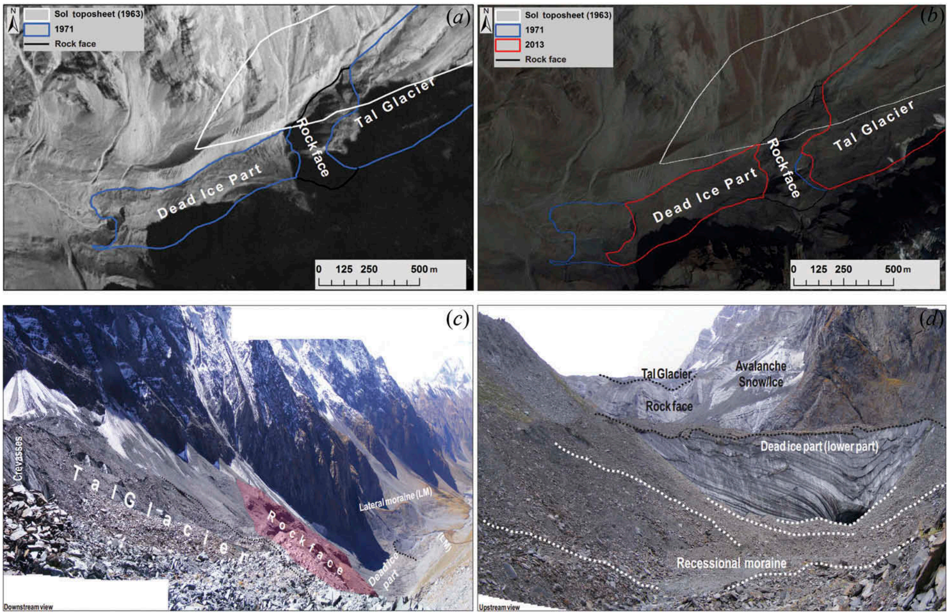

Figure 4. Recession of Tal Glacier, Budhil sub-basin of Ravi. (*a*) Corona KH-4A image (28 September 1971) with same-year glacier outline; (*b*) Google Earth (GE) image (26 September 2013) with glacier outline for 1971 and 2013 (Note: GE image used to show the location of snout and comparison when mapped in field, September, 2013); (*c*) field photographs showing (above) lower part of the glacier as the snout of the main Tal Glacier trunk; (lower right) dead ice part, 2013; (*d*) field photographs showing upper part of the glacier (2013) with the upper main trunk in background and lower dead ice part in the foreground.

This study demonstrates a highly erroneous rate of recession (123 m year^{-1}) and area vacated (0.6 km^2) for Manimahesh Glacier in comparison to the SoI map (1968) with Corona data (1971). Such a drastic reduction in size and higher rate of recession is simply impossible within just 3 years and thus suggests misinterpretation of the glacier boundary from the SoI topographic map. In addition, field measurements and geomorphological mapping of the deglaciated area, and a high-resolution Corona image (1971), show that the glacier outline derived from the SoI topographical map (1968) includes an area near the moraine contemporaneous with LIA on the basis of mapped moraine extent in the field (Figures 3(*c*) and 5). In addition, the glacier of an adjoining basin is included in the SoI map (1968) of the accumulation area of Manimahesh Glacier, thus providing a highly overestimate figure in terms of total glacier area (Figure 5). This indicates that the greater retreat of Manimahesh Glacier provided previously was probably due to overestimation in delineating the glacier outline from the SoI map (1968). Therefore, SoI maps from the 1960s–70s must be used with caution in regard to changes in glacier front and overall morphology.

This study reports that the clean-ice-covered Manimahesh Glacier has a strong correlation with total higher percentage glacial area loss as compared with the debris-covered Tal Glacier, which is consistent with results for other glaciated regions across the Himalaya (Scherler, Bookhagen, and Strecker 2011; Bolch et al. 2008; Bhambri et al. 2011; Bahuguna et al. 2014). However, less recession and area loss is reported for glaciers with extensive debris cover, because it is proposed that thick debris cover on glaciers

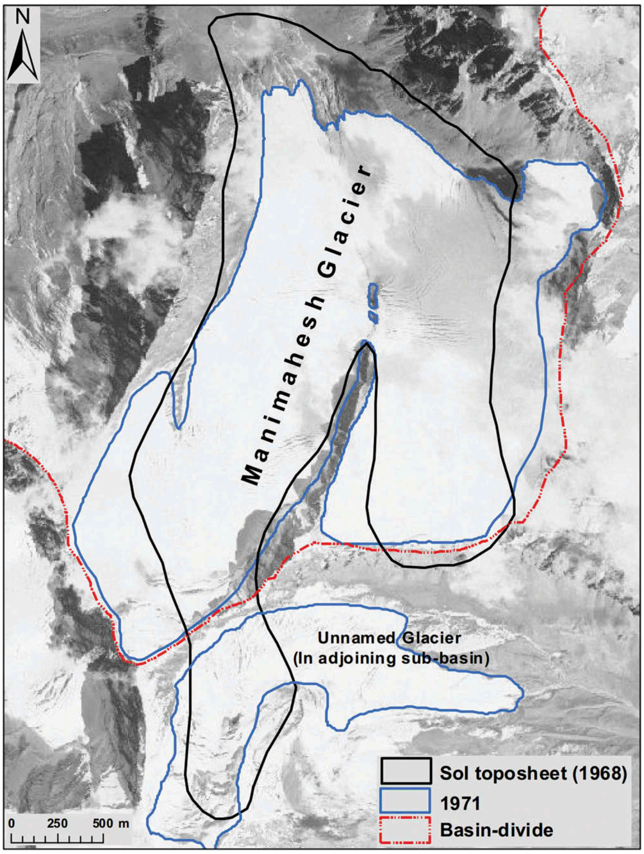

Figure 5. Manimahesh Glacier outlines for 1968 (SoI toposheet) and 1971 (Corona KH-4A image). Note the error in the SoI toposheet as the glacier outlines cross the ridges and its accumulation area.

leads, in general, to less frontal retreat or even stable tongues, as the rate of surface melting is reduced (Benn and Owen 2002; Benn et al. 2012). This needs further detailed investigations.

An earlier study by GSI (Shukla and Dutta 2005) calculated the extent of retreat along the central flow line or more or less along the melted stream from the terminus. The present study, taking the average length from the intersection of the stripes, yields a recession for Manimahesh Glacier of 157 ± 34 m between 1971and 2013. Recession along the average central flow line was 212 ± 34 m during this period. These findings show varying tendencies attributed to the curvilinear shape of the central flow line; further measurements based only on single points of the glacier may result in overestimation of recession, and are more susceptible to outliers (Bhambri, Bolch, and Chaujar 2012). Averaging along the front is a more robust method and provides more reliable estimations, especially in the situation of a change in location of clean-ice-covered glaciers with no well-defined snout or terminus. The rate of retreat of glacial length and discrepancy in total areal loss may possibly be due to glacier margin morphology. Furthermore, the frontal width–length ratio is affected due to the greater width of the frontal part of the Manimahesh Glacier terminus, which yields a higher areal loss with lower terminus recession (Figures 3(*b*) and 5).

5. Discussion

The areal changes of the glaciers in the Ravi basin confirm an expected and published trend of glacial retreat (Shukla and Dutta 2005). However, the rate of retreat is less than those previously estimated from SoI topographic map analyses: 29 and 40 m year^{-1} for Manimahesh and Tal Glaciers, respectively. In addition, the recession rate for debris-covered glaciers (Tal Glacier, 1 ± 1 m year^{-1}) in the Ravi basin is also comparatively lower than for other glaciers in Himachal Himalaya using SoI topographic maps (e.g. Samudra Tapu (20 m year^{-1}), Chhota Shigri (7 m year^{-1}), Parbati (168.4 m year^{-1}), Sara-Umga (41 m year^{-1}), Bara-Shigri (30 m year^{-1}), and Miyar (17 m year^{-1}) (Kulkarni and Karyakarte 2014) (Figure 6)). The reason for this discrepancy is probably the interpretation of the glacier terminus on SoI topographic maps, which is known to be a significant challenge in glacier terminus mapping (Bhambri and Bolch 2009). Moreover, the long-term rate of retreat for the previous 40 years is available for around 100 glaciers in the Himalaya (Kulkarni and Karyakarte 2014; Bolch et al. 2012). The reported mean loss of glacial length over four decades is approximately 621 ± 468 m, with large variations across the Himalayan region (Kulkarni and Karyakarte 2014). This is many times (4–13) higher than the average rate of retreat calculated for Manimahesh (157 ± 34 m) and Tal (45 ± 34 m). The same retreat trend was reported for glaciers in the Garhwal Himalaya (e.g. Gangotri (20 m year^{-1}), Millam (25 m year^{-1}), Dokriani (15 m a year^{-1}), Tipra (14 m year^{-1}), Chorabari (6 m year^{-1}), Pindari (6 m year^{-1}), Satopanth (23 m year^{-1}), and Bhagirath-Kharak (7 m year^{-1})) based on SoI topographic maps and remote-sensing data with limited field observations (Bhambri, Bolch, and Chaujar 2012; Mehta et al. 2014; Nainwal et al. 2008; Raj 2011). Additionally, changes in glacier terminus and area were observed in other Himalayan regions (e.g. Drang-Drung (9 m year^{-1}) in the Jammu

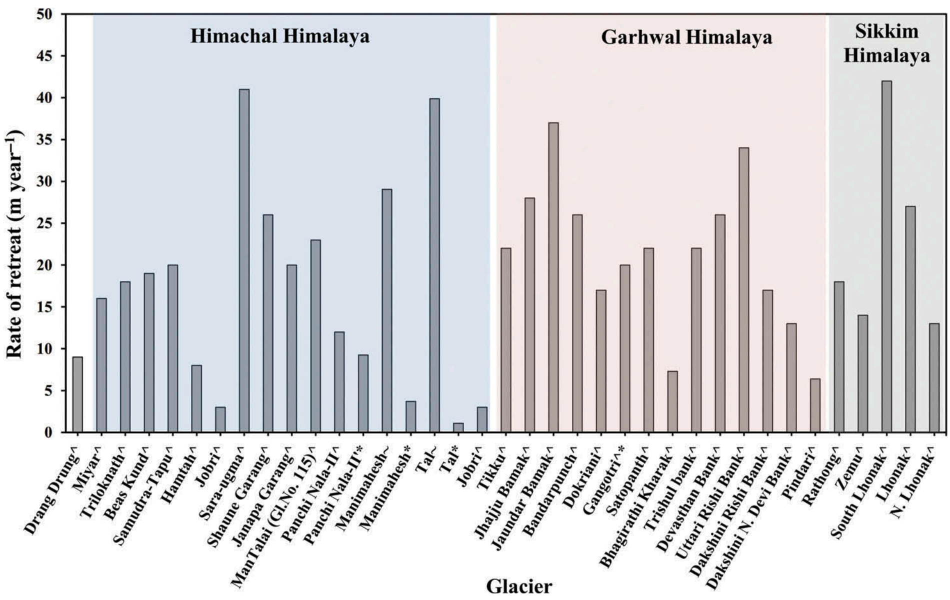

Figure 6. Glacier terminus change trends in Indian Himalaya (^Kulkarni and Karyakarte 2014; ~Shukla and Dutta 2005; !Negi et al. 2013). Note that comparison of recession rate for similar glaciers (Manimahesh, Tal, Panchi Nala-II) derived from SoI topographical maps and Corona data* shows significant differences.

and Kashmir region; Rekha-Samb (12 m year^{-1}) in Nepal; and Zemu (14 m year^{-1}), South Lhonak (42 m year^{-1}), and Rathong (18 m year^{-1}) in Sikkim (Kulkarni and Karyakarte 2014)). These glaciers show a retreating trend over recent decades (Figure 6). However, glaciers in the western, central, and eastern Karakoram show long-term irregular behaviour with frequent advances and possible slight mass gain mainly since 2000 (Hewitt 2011; Bolch et al. 2012; Kääb et al. 2012; Gardelle et al. 2013; Bhambri et al. 2013; Schmidt and Nüsser 2009). Therefore, regional irregularity in Himalayan glacier fluctuation represents an unusual behaviour. Further detailed study is therefore required on glacial fluctuation in inadequately observed basins across the Himalaya.

Earlier studies on the estimation of glacial area and recession for the Indian Himalaya are based on SoI maps (1960s–70s) and coarser-resolution satellite images (Kulkarni et al. 2007; Mir et al. 2014; Pandey and Venkataraman 2013; Pandey, Ghosh, and Nathawat 2011; Kulkarni and Rathore 2005; Mehta, Dobhal, and Bisht 2011; Mehta et al. 2014). The present study suggests that earlier estimations primarily based on SoI maps are highly erroneous and overestimate glacial change, and therefore reassessment and recalculation, if possible, are required for more accurate and pragmatic results. Inaccuracies in delineating glacial boundaries in SoI topographic maps have previously been reported (Bhambri and Bolch 2009). Interestingly, Ahmad et al. (2004) estimated a 10 km^2 vacation of the Gangotri glacier between 1985 and 2001, based on topographic maps and satellite imagery – an overestimation of around 24-fold (0.41 ± 0.03 km^2) as reported by Bhambri, Bolch, and Chaujar (2012) using high-resolution satellite data sets. Bhambri and Bolch (2009) reported an areal change of 3.7 km^2 for Parbati glacier over 25 years, based on comparison of SoI topographic maps from 1962 and 1987, which is almost twofold lower than the 8.3 km^2 reported by Kulkarni and Rathore (2005) over 28 years based on the 1962 SoI topographic map and a 1990 satellite image. Declassified high-spatial resolution Corona imagery acquired during the same period as the SoI map upgrades of the 1960s and 1970s has the potential to derive accurate past/historic glacial outlines for comparison with contemporary outlines and dynamics.

6. Conclusion

This study shows that between 1971 and 2013, the Manimahesh and Tal Glaciers retreated by 157 ± 34 m (4 ± 1 m year^{-1}) and 45 ± 34 m (1 ± 1 m year^{-1}), respectively, and the total area lost is estimated at 0.21 ± 0.01 km^2 (0.005 km^2 year^{-1}) and 0.010 ± 0.003 km^2 (0.0002 km^2 year^{-1}), respectively. Our results suggest that the rate of retreat for these glaciers is many times (7- and 37-fold for Manimahesh and Tal, respectively) lower than previously reported (Shukla and Dutta 2005). Insignificant changes are observed for the debris-covered Tal Glacier over that timeframe. However, our study does not imply that glacier recession in the Ravi basin has ceased. Linear or areal changes in the frontal part of glaciers show only the indirect and delayed response to climate change, in contrast to their mass balance. Moreover, the rate of recession of Tal Glacier is low compared with other glaciers, probably due to topographic configuration and the effects of thick supraglacial debris. The response time to melting and change for such extensively debris-covered glaciers (e.g. Tal Glacier) is probably much longer than that of smaller or clean-ice-covered glaciers. Thus, a study of long-term glaciological mass balance is key to deriving a precise assessment of glacial health. However, *in situ* measurements are logistically difficult in such terrain and hence not feasible owing to glacial size and characteristics. The geodetic approach using Corona data may represent a more suitable and cost-effective method. Moreover, topographic parameters such as elevation range, mean elevation, and aspect, as well as glacial morphology, size, velocity, thickness, and distribution of debris-covered area, need to be addressed along with others parameters for any future studies.

The main challenges with the use of Corona data are the complex image geometry and absence of satellite camera specifications, which can be resolved by the availability of recent techniques or software to maintain and enhance the positional accuracy of rectified imagery based on unchanged location points and field GCPs. This study strongly recommends the use of declassified Corona images of the 1960s–70s to re-examine glacial change, particularly in the Indian Himalaya, where SoI maps were previously used extensively for glacial change detection. Such analysis would provide more representative or accurate values/results for glacial fluctuation, and change a poorly conceived perception of high melt and retreat of Himalayan glaciers, hitherto incorrectly presented, using incomparable data sets.

Acknowledgements

The authors are grateful to Jawaharlal Nehru University, New Delhi, for providing the research facilities. We also thank the USGS for providing Landsat TM/ETM+/OLI and Corona data. The first author is grateful to Mr Bruce Raup, GLIMS (http://www.glims.org/), for providing ASTER satellite data at no cost. The first author also extends his gratitude to Dr Rakesh Bhambri for valuable suggestions. The authors extend their gratitude to Dr Timothy Warner, Editor, IJRS, for his insightful comments and suggestions, which significantly improved the flow and content of this article.

Disclosure statement

No potential conflict of interest was reported by the authors.

Funding

We are grateful to the University Grant Commission, New Delhi, for financial support for this work.

ORCID

Pritam Chand http://orcid.org/0000-0001-7388-0393

References

Ahmad, S., S. I. Hasnain, C. D. Arha, V. S. Ramamurthy, K. N. Mathur, and U. K. Bassi. 2004. "Analysis of Satellite Imageries for Characterization of Glacio-Morphological Features of the Gangotri Glacier, Ganga Headwater, Garhwal Himalaya." *Proceedings of Workshop on Gangotri Glacier Special Publication Series-Geological Survey of India* 80: 61–67.

Azam, M. F., P. Wagnon, A. Ramanathan, C. Vincent, P. Sharma, Y. Arnaud, A. Linda, J. G. Pottakkal, P. Chevallier, V. B. Singh, and E. Berthier. 2012. "From Balance to Imbalance: A Shift in the Dynamic Behaviour of Chhota Shigri Glacier, Western Himalaya, India." *Journal of Glaciology* 58 (208): 315–324. doi:10.3189/2012JoG11J123.

Bahuguna, I. M., B. P. Rathore, R. Brahmbhatt, M. Sharma, S. Dhar, S. S. Randhawa, K. Kumar, S. Romshoo, R. D. Shah, R. K. Ganjoo, and Ajai. 2014. "Are the Himalayan Glaciers Retreating?" *Current Science* 106 (7): 1008–1013.

Beck, A., G. Philip, M. Abdulkarim, and D. Donoghue. 2007. "Evaluation of Corona and Ikonos High Resolution Satellite Imagery for Archaeological Prospection in Western Syria." *Antiquity* 81 (311): 161–175. doi:10.1017/S0003598X00094916.

Benn, D. I., T. Bolch, K. Hands, J. Gulley, A. Luckman, L. I. Nicholson, D. Quincey, S. Thompson, R. Toumi, and S. Wiseman. 2012. "Response of Debris-Covered Glaciers in the Mount Everest

Region to Recent Warming, and Implications for Outburst Flood Hazards." *Earth-Science Reviews* 114 (1–2): 156–174. Elsevier B.V. doi:10.1016/j.earscirev.2012.03.008.

Benn, D. I., and L. A. Owen. 2002. "Himalayan Glacial Sedimentary Environments: A Framework for Reconstructing and Dating the Former Extent of Glaciers in High Mountains." *Quaternary International* 97–98 (January): 3–25. doi:10.1016/S1040-6182(02)00048-4.

Bhagat, R., V. Kalia, C. Sood, P. K. Mool, and S. R. Bajracharya. 2004. *Inventory of Glaciers, Glacial Lakes and Identification of Potential Glacial Lake Outburst Floods (GLOFs) Affected by Global Warming in the Mountains of Himalayan Region*. Kathmandu: ICIMOD (International Centre for Integrated Mountain Development).

Bhambri, R., and T. Bolch. 2009. "Glacier Mapping: A Review with Special Reference to the Indian Himalayas." *Progress in Physical Geography* 33 (5): 672–704. doi:10.1177/0309133309348112.

Bhambri, R., T. Bolch, and R. K. Chaujar. 2012. "Frontal Recession of Gangotri Glacier, Garhwal Himalayas, from 1965 to 2006, Measured through High- Resolution Remote Sensing Data." *Current Science* 102 (3): 1462–1466.

Bhambri, R., T. Bolch, and R. K. Chaujar. 2010. "Glacier Mapping in India since the 19th Century." *The Himalayan Journal* 66: 173–182.

Bhambri, R., T. Bolch, R. K. Chaujar, and S. C. Kulshreshtha. 2011. "Glacier Changes in the Garhwal Himalaya, India, from 1968 to 2006 Based on Remote Sensing." *Journal of Glaciology* 57 (203): 543–556. doi:10.3189/002214311796905604.

Bhambri, R., T. Bolch, P. Kawishwar, D. P. Dobhal, D. Srivastava, and B. Pratap. 2013. "Heterogeneity in Glacier Response in the Upper Shyok Valley, Northeast Karakoram." *The Cryosphere* 7 (5): 1385–1398. doi:10.5194/tc-7-1385-2013.

Bolch, T., M. Buchroithner, T. Pieczonka, and A. Kunert. 2008. "Planimetric and Volumetric Glacier Changes in the Khumbu Himal, Nepal, since 1962 Using Corona, Landsat TM and ASTER Data." *Journal of Glaciology* 54 (187): 592–600. doi:10.3189/002214308786570782.

Bolch, T., A. Kulkarni, A. Kaab, C. Huggel, F. Paul, J. G. Cogley, and H. Frey, J. S. Kargel, K. Fujita, M. Scheel, S. Bajracharya, and M. Stoffel. 2012. "The State and Fate of Himalayan Glaciers." *Science (New York, N.Y.)* 336 (6079): 310–314. doi:10.1126/science.1215828.

Bolch, T., T. Yao, S. Kang, M. F. Buchroithner, D. Scherer, F. Maussion, E. Huintjes, and C. Schneider. 2010. "A Glacier Inventory for the Western Nyainqentanglha Range and the Nam Co Basin, Tibet, and Glacier Changes 1976–2009." *The Cryosphere* 4 (3): 419–433. Copernicus GmbH. doi:10.5194/tc-4-419-2010.

Bolch, T., B. Menounos, and R. Wheate. 2010. "Landsat-Based Inventory of Glaciers in Western Canada, 1985–2005." *Remote Sensing of Environment* 114 (1): 127–137. doi:10.1016/j.rse.2009.08.015.

Csatho, B. M., C. J. Van Der Veen, and C. M. Tremper. 2005. "Trimline Mapping from Multispectral Landsat ETM+ Imagery." *Géographie Physique Et Quaternaire* 59 (1): 49. Les Presses de l'Université de Montréal. doi:10.7202/013736ar.

Dobhal, D. P., M. Mehta, and D. Srivastava. 2013. "Influence of Debris Cover on Terminus Retreat and Mass Changes of Chorabari Glacier, Garhwal Region, Central Himalaya, India." *Journal of Glaciology* 59 (217, International Glaciological Society): 961–971. doi:10.3189/2013JoG12J180.

Frey, H., F. Paul, and T. Strozzi. 2012. "Compilation of a Glacier Inventory for the Western Himalayas from Satellite Data: Methods, Challenges, and Results." *Remote Sensing of Environment* 124 (September): 832–843. doi:10.1016/j.rse.2012.06.020.

Gardelle, J., E. Berthier, Y. Arnaud, and A. Kääb. 2013. "Region-Wide Glacier Mass Balances over the Pamir-Karakoram-Himalaya during 1999–2011." *The Cryosphere* 7 (4): 1263–1286. doi:10.5194/tc-7-1263-2013.

Granshaw, F. D., and A. G. Fountain. 2006. "Glacier Change (1958–1998) in the North Cascades National Park Complex, Washington, USA." *Journal of Glaciology* 52 (177): 251–256. doi:10.3189/172756506781828782.

Hall, D. K., K. J. Bayr, W. Schöner, R. A. Bindschadler, and J. Y. L. Chien. 2003. "Consideration of the Errors Inherent in Mapping Historical Glacier Positions in Austria from the Ground and Space (1893–2001)." *Remote Sensing of Environment* 86 (4): 566–577. doi:10.1016/S0034-4257(03)00134-2.

Hewitt, K. 2011. "Glacier Change, Concentration, and Elevation Effects in the Karakoram Himalaya, Upper Indus Basin." *Mountain Research and Development* 31 (3): 188–200. International Mountain Society. doi:10.1659/MRD-JOURNAL-D-11-00020.1.

Kääb, A., E. Berthier, C. Nuth, J. Gardelle, and Y. Arnaud. 2012. "Contrasting Patterns of Early Twenty-First-Century Glacier Mass Change in the Himalayas." *Nature* 488 (7412): 495–498. Nature Publishing Group, a division of Macmillan Publishers Limited. All Rights Reserved. doi:10.1038/nature11324.

Kulkarni, A. V., I. M. Bahuguna, B. P. Rathore, S. K. Singh, S. S. Randhawa, R. K. Sood, S. Dhar, and others. 2007. "Glacial Retreat in Himalaya Using Indian Remote Sensing Satellite Data." *Current Science* 92 (1): 69–74.

Kulkarni, A. V., and Y. Karyakarte. 2014. "Observed Changes in Himalayan Glaciers." *Current Science* 106 (2): 237–244. Current Science Association.

Kulkarni, A. V., and B. P. Rathore. 2005. "Alarming Retreat of Parbati Glacier, Beas Basin, Himachal Pradesh." *Current Science* 88 (11): 1844–1850.

Mayewski, P. A., and P. A. Jeschke. 1979. "Himalayan and Trans-Himalayan Glacier Fluctuations Since AD 1812." *Arctic and Alpine Research* 11 (3): 267–287. doi:10.2307/1550417.

Mehta, M., D. P. Dobhal, and M. P. S. Bisht. 2011. "Change of Tipra Glacier in the Garhwal Himalaya, India, between 1962 and 2008." *Progress in Physical Geography* 35 (6): 721–738. doi:10.1177/0309133311411760.

Mehta, M., D. P. Dobhal, K. Kesarwani, B. Pratap, A. Kumar, and A. Verma. 2014. "Monitoring of Glacier Changes and Response Time in Chorabari Glacier, Central Himalaya, Garhwal, India." *Current Science* 107 (2): 281–289. Indian Acad Sciences.

Mir, R. A., S. K. Jain, A. K. Saraf, and A. Goswami. 2014. "Glacier Changes Using Satellite Data and Effect of Climate in Tirungkhad Basin Located in Western Himalaya." *Geocarto International* 29 (3): 293–313. Taylor & Francis. doi:10.1080/10106049.2012.760655.

Nainwal, H. C., B. D. S. Negi, M. Chaudhary, K. S. Sajwan, and A. Gaurav. 2008. "Temporal Changes in Rate of Recession: Evidences from Satopanth and Bhagirath Kharak Glaciers, Uttarakhand, Using Total Station Survey." *Current Science* 94 (5): 653–660.

Negi, H. S., G. Saravana, R. Rout, and Snehmani. 2013. "Monitoring of Great Himalayan Glaciers in Patsio Region, India Using Remote Sensing and Climatic Observations." *Current Science* 105 (10): 1383–1392.

Pandey, A. C., S. Ghosh, and M. S. Nathawat. 2011. "Evaluating Patterns of Temporal Glacier Changes in Greater Himalayan Range, Jammu & Kashmir, India." *Geocarto International* 26 (4): 321–338. doi:10.1080/10106049.2011.554611.

Pandey, P., and G. Venkataraman. 2013. "Changes in the Glaciers of Chandra–Bhaga Basin, Himachal Himalaya, India, between 1980 and 2010 Measured Using Remote Sensing." *International Journal of Remote Sensing* 34 (15): 5584–5597. Taylor & Francis. doi:10.1080/01431161.2013.793464.

Pareta, K., and U. Pareta. 2014. "Climate Change Impact on Land and Natural Resource in Chamba Tehsil of Himachal Pradesh State, India." *The International Journal of Science & Technoledge* 2 (4): 38–48.

Paul, F., N. E. Barrand, S. Baumann, E. Berthier, T. Bolch, K. Casey, and H. Frey, S. P. Joshi, V. Konovalov, R. L. Bris, N. Mölg, G. Nosenko, C. Nuth, A. Pope, A. Racoviteanu, P. Rastner, B. Raup, K. Scharrer, S. Steffen, and S. Winsvold. 2013. "On the Accuracy of Glacier Outlines Derived from Remote-Sensing Data." *Annals of Glaciology* 54 (63): 171–182. International Glaciological Society. doi:10.3189/2013AoG63A296.

Paul, F., H. Frey, and R. Le Bris. 2011. "A New Glacier Inventory for the European Alps from Landsat TM Scenes of 2003: Challenges and Results." *Annals of Glaciology* 52 (59): 144–152. doi:10.3189/172756411799096295.

Paul, F., A. Kääb, M. Maisch, T. Kellenberger, and W. Haeberli. 2002. "The New Remote-Sensing-Derived Swiss Glacier Inventory: I. Methods." *Annals of Glaciology* 34 (1): 355–361. International Glaciological Society. doi:10.3189/172756402781817941.

Paul, F., and F. Svoboda. 2009. "A New Glacier Inventory on Southern Baffin Island, Canada, from ASTER Data : II. Data Analysis, Glacier Change and Applications." *Annals of Glaciology* 50 (53): 22–31.

Racoviteanu, A. E., F. Paul, B. Raup, S. J. S. Khalsa, and R. Armstrong. 2009. "Challenges and Recommendations in Mapping of Glacier Parameters from Space : Results of the 2008 Global

Land Ice Measurements from Space (GLIMS) Workshop, Boulder, Colorado, USA." *Annals of Glaciology* 50 (53): 53–69. doi:10.3189/172756410790595804.

Racoviteanu, A. E., M. W. Williams, and R. G. Barry. 2008. "Optical Remote Sensing of Glacier Characteristics: A Review with Focus on the Himalaya." *Sensors* 8 (5): 3355–3383. doi:10.3390/s8053355.

Raina, V. K., and D. Srivastava. 2008. *Glacier Atlas of India*. Bangalore: Geological Society of India (GSI).

Raj, K. B. G. 2011. "Recession and Reconstruction of Milam Glacier, Kumaon Himalaya, Observed with Satellite Imagery." *Current Science* 100 (9): 1420–1425.

Raju, P. P., and S. Ghosh. 2003. "Role of Remote Sensing and Digital Cartography in Sustainable Development." *Indian Cartographer* 23: 88–95.

Scherler, D., B. Bookhagen, and M. R. Strecker. 2011. "Spatially Variable Response of Himalayan Glaciers to Climate Change Affected by Debris Cover." *Nature Geoscience* 4 (3): 156–159. Nature Publishing Group. doi:10.1038/ngeo1068.

Schmidt, S., and M. Nüsser. 2009. "Fluctuations of Raikot Glacier during the Past 70 Years: A Case Study from the Nanga Parbat Massif, Northern Pakistan." *Journal of Glaciology* 55 (194): 949–959. International Glaciological Society. doi:10.3189/002214309790794878.

Shukla, S. P., and S. S. Dutta. 2005. *Generation of Baseline Data on Secular Movement of Selected Glaciers in Ravi Basin, Chamba District, Himachal Pradesh (Tal and Manimahesh Glaciers)*. Lucknow: Geological Survey of India (GSI).

Slaymaker, O., and R. Kelly. 2007. *The Cryosphere and Global Environmental Change*. Wiley. http://books.google.co.in/books/about/The_Cryosphere_and_Global_Environmental.html?id=1ftZeYFGaYoC&pgis=1.

Spate, O. H. K., and A. T. A. Learmonth. 1967. *India and Pakistan- A General and Regional Geography*. London: Methuen.

Zemp, M., I. Roer, A. Kääb, M. Hoelzle, F. Paul, and W. Haeberli. 2008. *Global Glacier Changes : Facts and Figures Contents*. Zurich: UNEP, World Glacier Monitoring Service (WGMS).

International Journal of Remote Sensing 2015.36:4095-4113.